A deamination-driven biocatalytic cascade for the synthesis of ribose-1-phosphate
Supplementary Information

Jonas Motter[1], Sarah Westarp[1,2], Jonas Barsig[1], Christina Betz[1], Amin Dagane[1], Felix Kaspar[1,4], Lena Neumair[1], Sebastian Kemper[3], Peter Neubauer[1], and Anke Kurreck[1,2*]

[1]Chair of Bioprocess Engineering, Institute of Biotechnology, Faculty III Process Sciences, Technische Universität Berlin, Ackerstraße 76, 13355 Berlin, Berlin, Germany

[2]BioNukleo GmbH, Ackerstraße 76, 13355 Berlin, Germany

[3]Institute for Chemistry, Technische Universität Berlin, Straße des 17. Juni 135, 10623 Berlin, Germany

[4]Institute for Biochemistry, Biotechnology and Bioinformatics, Technische Universität Braunschweig, Spielmannstraße 7, 38106, Braunschweig, Germany

*Correspondence: anke.wagner@tu-berlin.de

Contents

Experimental information

General information

All chemicals and solvents were of analytical grade or higher, used without further purification and purchased from Sigma-Aldrich (Steinheim, Germany), Carl Roth (Karlsruhe, Germany), TCI Deutschland (Eschborn, Germany), Biosynth (Berkshire, UK), or VWR (Darmstadt, Germany). The purine nucleoside phosphorylases (PNP N02, E-NP-2002, CAS Number 9030-21-1, and PNP N04, E-NP-2004, CAS Number 9030-21-1) and pyrimidine nucleoside phosphorylase (PyNP Y02, E-NP-1002, CAS Number 9055-35-0) were kindly provided by BioNukleo GmbH (Berlin, Germany). Stock solutions with concentrations usually between 1 mM and 5 mM for nucleosides and 50 mM for **Rib1P** were prepared in deionised water (prepared with a Veolia purification system). Nucleosides and nucleobases were stored at room temperature (as precipitation routinely occurred at 4 °C), and **Rib1P** was stored at –20 °C to protect from degradation. All raw MS and NMR data, as well as each figure's source data (when applicable) from the main manuscript and SI, are freely available externally at zenodo.org (ref[1]).

Bioinformatic and database

Sequences are available from UniProt (https://www.uniprot.org/) and PDB (https://www.rcsb.org/). Alignment was performed using the Clustal2.1 tool. Structural prediction was performed using AlphaFold (https://alphafold.ebi.ac.uk/) and superimposition via the PDB structural alignment tool (https://www.rcsb.org/alignment, jFATCAT (rigid)). Please see the respective sections in this supplementary information for accessions and sequences.

Cloning and transformation

Guanine deaminase gene of *Deinococcus geothermalis* (*Dg*GuaD) was synthesised by GeneArt (ThermoFisher, Darmstadt, Germany) with BamHI and HindIII restriction sites. We first transformed competent cells (*E. coli* Top10) to amplify the GeneArt plasmid. To introduce an N-terminal *His*$_6$-tag for purification and enable inducible expression under the control of the lac-operon, we cloned the gene of interest into an expression vector (a modified pCTUT7, a plasmid map can be found in ref[2]) using the restriction sites BamHI and HindIII.

All **transformations** were performed with the following procedure: *E. coli* pellet of a 10 mL culture grown in LB medium for 1 h at 37 °C and 250 rpm was washed in an ice-cold solution of 50 mM Tris pH 7.5 /0.1 M $CaCl_2$ twice and incubated on ice for 30 min in the first wash and 2 h in the second wash step (final volume 600 µL). 100 µL of the chemically competent cells were incubated on ice for 30 minutes with 1 µL of either plasmid or ligation mix. The cells were then heat-shocked at 42 °C for 1 min, and 600 µL of SOC medium was added before shaking the

transformation mix at 37 °C for 1 h. Subsequently, the cells harbouring the plasmids were streaked on LB plates with 1% ampicillin (the resistance is transferred by the plasmid).

Plasmid purification: Cells carrying the plasmid were incubated in 5 mL LB for 6 h at 37 °C and 250 rpm. The cells were harvested by centrifugation and lysed, and the plasmid was purified using the QIAprep® Spin Miniprep Kit.

Cloning procedure: The obtained plasmids (amplicons of the GeneArt vector) were cut with BamHI and HindIII (Cutsmart, 5 µL of plasmid was combined with 5 µL of buffer, 37 µL of water, 1µL BamHI and 2 µL of HindIII). The amount of HindIII was twice used, as the enzyme only showed 50% activity in the buffer, while BamHI showed 100% activity in Cutsmart. The restriction was run at 37 °C for 1 h. In the last 5 minutes of the restriction, phosphatase was added to prevent the re-ligation of the insert with the rest of the plasmid. After manufacturing recommendations, the insert was isolated via agarose gel electrophoresis (2% agarose) and purified via QIAquick Gel Extraction Kit. Next, we cloned the insert into the expression vector by combining the backbone to insert in a 1:3 ratio. The ligation was performed in a total volume of 50 µL containing 5 µL buffer, 1 µL ligase, and 34 µL water for 1.5 h. Following the abovementioned procedure, the plasmid was introduced into competent BL21 cells and then plated onto LB agar plates with 100 µg mL^{-1} ampicillin and 1% glucose. Glucose was added to prevent any leaky expression from the plasmid. The sequence of the obtained plasmid was verified by Sanger Sequencing (LGC Genomics GmbH).

Expression and purification of the used enzymes

*Dg*GuaD was expressed in *E. coli* BL21 (NEB, Frankfurt am Main, Germany) using EnPresso® B medium (Enpresso, Berlin, Germany) based on the manufacturer's recommendations and as recently described.[3,4] Briefly, 50 mL Enpresso B medium supplemented with antibiotic (100 mg L^{-1} ampicillin) was inoculated to an initial OD_{600} of 0.15 in an Ultra Yield flask (250 mL). The resulting culture was grown at 30 °C and 200 rpm for 15-18 h before adding Isopropyl-β-D-thiogalactopyranosid (IPTG) to a final concentration of 0.1 mM. The culture was incubated at 30 °C and 250 rpm for 24 h before the cells were harvested by centrifugation (8000 g, 10 min, 4 °C). The cell pellet was frozen or used for lysis directly (see below).

To perform lysis and purification, the cells were subjected to an enzymatic lysis buffer containing 0.6 µg mL^{-1} DNA Benzonase (Merck), 1 mg mL^{-1} Lysozyme (Fluke), and 1 mM $MgCl_2$. The cells were incubated with a buffer-to-wet weight ratio of 3 mL per gram at room temperature for 30 min. The cells were then disrupted using sonication (10 min at 30% power input and 30 seconds on/off intervals). Consequently, the resulting lysate was treated at a temperature of 50 °C for 20-30 minutes to precipitate *E. coli* proteins and cell debris. After that, the precipitated protein was separated by centrifugation (8000 g, 20 min, 4°C). Cell-free extracts were then applied to a Ni Sepharose column (Jena Bioscience) pre-equilibrated with a binding buffer (50 mM sodium phosphate buffer, 300 mM NaCl, 10 mM imidazole). Non-specifically binding proteins were eliminated by a washing buffer (50

mM sodium phosphate buffer, 300 mM NaCl, 20 mM imidazole). The protein of interest was finally eluted with an elution buffer (50 mM sodium phosphate buffer, 300 mM NaCl, 250 mM imidazole). Fractions containing pure target protein (as determined by 12%-SDS PAGE) were combined and directly subjected to dialysis against 2 mM K_2HPO_4 (pH 9). The resulting protein preparations were stored at 4 °C. The purity of enzyme preparation was checked via SDS-PAGE (12%). Protein concentration was determined by A280 measurements at a ThermoFisher Scientific NanoDrop One using the molar extinction coefficient E1% predicted by Protparam.

Enzymatic reactions

Enzymatic reactions typically were conducted in a volume of 200 µL to 2000 µL. Reactions were usually prepared from stock solutions except for reactions containing >5 mM **Guo**. After adding the enzyme, reactions were typically incubated in a water bath (in glass reaction vials, up to 4 mL), thermoblock (in reactions up to 2 mL), or PCR cycler (in reactions up to 200 µL), depending on the reaction volume. Pictures of the experimental setup can be found in *Figure S12*. Samples were drawn for spectral unmixing, HPLC, or TLC (see below). For detailed information on supplementary experiments, see their respective figure descriptions.

Kinetic reactions for GuaD dependent on the pH value were performed with 1 mM **Gua**, 50 mM K_2HPO_4, 50 mM PHB buffer with different pH values, and 10 µL enzyme in a total reaction volume of 500 µL. Reactions were drawn and analysed via HPLC. Reactions were carried out at four different temperatures to determine how temperature influences activity. The specific activity was determined based on the initial reaction velocity, where one unit (U) is one micromole substrate conversion per minute. The temperatures investigated were 30 °C, 40 °C, 50 °C and 60 °C. The total reaction volume was 400 µL for all measurements, and 50 mM glycine-OH pH 9 (pH was adjusted with KOH or NaOH) and 0.2 mM **Gua** were used. The enzyme concentration was set to 0.08 µg mL^{-1} at 30 °C for two measurements and halved with increasing temperature. This means that 0.04 µg mL^{-1} was used at 40 °C, 0.02 µg mL^{-1} at 50 °C and 0.01 µg mL^{-1} at 60 °C. 70 µL samples were taken after 1, 2 and 3 min and quenched in 140 µL 200 mM NaOH for analysis via spectral unmixing. Based upon this, we calculated the observed rate constant (k_{obs}) as the degree of conversion (mol per second) per mol enzyme applied (using the molar extinction coefficient as predicted by Protpram). All kinetic experiments were conducted in triplicates.

To investigate whether *Dg*GuaD also reacts with other nucleobases, reactions were prepared with a volume of 200 µL containing 50 mM glycine-OH pH 9, 1 µg mL^{-1} of the enzyme and 0.2 mM of the respective nucleobase. These reactions were incubated for 20 min at 40 °C. The absorbance was then measured between 250 and 350 nm and compared with a reference sample of the respective nucleoside.

To develop the biocatalytic cascades, the first screening reactions were performed in a volume of 200 µL containing 5 mM **Guo** with various concentrations of phosphate and enzyme concentration

(see main manuscript). Next, substrate-increased reactions (>5 mM) were performed in glass reaction vials with a magnetic stirrer in a volume of 2 mL and placed in a heated water bath at 50 °C. The same setup was applied for the pre-run of the gram synthesis under optimal conditions. Samples were typically analysed via TLC and HPLC.

Direct glycosylations with halogenated pyrimidine bases were performed with 2 mM **Rib1P**, 2 mM halogenated nucleobase, 50 mM glycine-OH pH 9, 0.1 mg mL^{-1} PyNP Y02 (BioNukleo GmbH, Berlin, Germany) in a total volume of 200 µL. Reactions were heated at 50 °C, and samples were drawn until they reached equilibrium as determined by HPLC.

Thermodynamic calculations were performed using the publicly available Excel sheet published in ref[5]. The readers are referred to the mentioned publication for the principles and background of those calculations.

Thermal shift assay

The melting temperature of *Dg*GuaD was measured using a thermal shift assay. Therefore, 100 µg mL^{-1} *Dg*GuaD was buffered in glycine-OH pH 9 (200 mM/50 mM) and MOPS pH 7 (200 mM/50 mM). The enzyme solutions were then heated to 50 °C for 30 seconds in a Biorad CFX96 Real-Time System. The temperature was increased in 0.5 °C increments every 5 s until a final temperature of 95 °C was reached. Fluorescence was measured during each 0.5 °C interval (λ_{ex} = 470 nm, λ_{em} = 570 nm). The melting temperature was determined as the inflexion point of fluorescence versus temperature.

Spectral unmixing

This UV/Vis spectroscopy-based method uses differences in UV absorption spectra of nucleosides and nucleobases after alkaline quenching to estimate their ratio based on spectral shape by fitting.[6] Samples for spectral unmixing were quenched with 2 equivalents (eq) NaOH, and UV absorption spectra volumes were recorded on a BioTek PowerWave HT plate reader using UV/Vis-transparent 96-well plates (UV-STAR F-Bottom #655801, Greiner Bio-One). Calculations were performed as previously shown.[7] The code is publicly available at https://gitlab.com/rgiessmann/data_toolbox.

High-performance liquid chromatography (HPLC)

For HPLC analysis, samples were stopped with 1 eq. ice-cooled MeOH. After centrifugation (21000 g, 25 min, 4 °C) to remove the enzyme, samples were analysed either on an Agilent 1200 or Agilent 1260 system. Here, we applied our previously published method[4,8] for separating reaction mixtures containing **Rib1P**, **Gua**, **Guo**, **Xan**, and **Xao**. The column temperature was set to 25 °C and separation was achieved on the Kinetex EVO C18 column (250 × 4.6 mm, Phenomenex) by applying a 1 mL min^{-1} flow with water (A) and MeCN (B) as eluent. The elution method consisted of a linear

gradient from 3–40% MeCN over 10 min, followed by 4 min re-equilibration at 3% MeCN. Chromatograms were extracted at 260 nm.

Optimised protocol for the gram-scale synthesis of Rib1P

After establishing a suitable method to produce **Rib1P**, two g-scale reactions were carried out according to the following scheme (*Figure S12A*):

i. The activity was validated using different PNP batches. This ensures that the reactions can be stopped at the highest conversion towards Rib1P and that the competing side reaction (**Xao** synthesis) can be kept at a minimum.

ii. Subsequently, a test synthesis was carried out on a 2 mL scale to estimate the optimal time to stop the reaction. Therefore, 25 mM **Guo** (1.06 g, 3.74 mmol) were reacted with 30 mM HPO_4^{2-} (1.2 eq., 4.5 mmol) and PNP N04 and *Dg*GuaD with the beforehand determined optimal enzyme concentration (0.049 mg mL^{-1} PNP N04 and 0.016 mg mL^{-1} *Dg*GuaD for the first run and 0.04 mg mL^{-1} PNP N04, 0.016 mg mL^{-1} *Dg*GuaD for the second run), at 50 °C. The reactions turned clear after ~15 min and reached ~88% conversion after 30-35 min.

iii. This was followed by the synthesis of **Rib1P** on a 150 mL scale (performed in round-bottom flasks) using the same reaction conditions as for the 2 mL reactions. Both batches' reactions were stopped after 30–35 min with 88% conversion. The reactions were stopped by freezing (–20 °C) in pre-cooled centrifugation tubes.

iv. Finally, purification was carried out by precipitation of nucleoside/base and phosphate. **Rib1P** was then precipitated as a barium salt. A detailed description of the purification can be found below.

While the first batch was used to optimize the workflow, the second batch served for the validation of our method. In the first batch, for example, the separation of the **Rib1P** precipitate by filtration or centrifugation was compared (Batch 1A and Batch 1B). Here, it was shown that centrifugation is more suitable but requires thorough drying to remove the EtOH. The data presented in the main manuscript are based on the results obtained for the second batch (Batch 2) unless stated otherwise.

Purification of Rib1P

For the purification of **Rib1P,** we modified our previously presented method.[9] After the enzymatic synthesis, the frozen reaction mixture was thawed, and the precipitated enzyme was removed by filtration through a cellulose nitrate filter (0.4 µm). All subsequent steps were performed on ice, and incubation steps were performed at 4 °C to protect **Rib1P** from degradation and facilitate precipitation. Next, the remaining nucleosides/nucleobases were precipitated by lowering the pH with HCl to ~7 (the measured value before was ~9.4–5). After incubation for 1 h, the reaction was filtered (cellulose nitrate filter, 0.4 µm). To raise the pH value again, an amount of aqueous ammonia solution (25% w/v) that corresponded to 1/3 of the volume of the reaction mixture was added. Phosphate was precipitated with a solution of $MgCl_2$ and NH_4Cl and was applied in a 1.5 eq.

concentration to the calculated remaining phosphate of the respective conversion. The solution was incubated for 3 h or overnight (16 h) and filtered (cellulose nitrate filter, 0.4 µm). Samples were drawn for TLC to verify phosphate precipitation. The filtrate was then used directly for barium precipitation. Barium acetate was added to the filtrate at an equimolar concentration (added in a 50 mL solution) compared to the nucleoside substrate, followed by 600 mL absolute ethanol addition. The barium salts of **Rib1P** were precipitated at 4 °C overnight (16–20 h). We compared filtration and centrifugation in the first synthesis, and these are annotated as Batch 1A and Batch 1B *(Figure 12D)*. Batch 2 originated from the second synthesis. The precipitated salts were collected by centrifugation at 8000 g for 10 min and filtrated samples with ethanol-compatible filters (>0.2 µM). The collected pellets were washed 2–3 times with absolute ethanol (>99.8%) and dried at 50 °C. The relative yield of **Rib1P**-Ba salts compared to the starting concentration of the substrate was calculated as the ratio of **Rib1P** concentration (mmol) to substrate concentration (**Guo**, mmol). Using standard curves, the purity of UV-active compounds was tested via HPLC at 260 nm. Overall purity was determined by quantitative ^{1}H measurements (see NMR spectroscopy). All yield and purity data are collected in *Figure S12*. Intactness was verified in direct glycosylations with halogenated uridine bases (see enzymatic reactions). A detailed description of the method can also be found in the greenness evaluation part.

Thin layer chromatography (TLC)

TLC analysis was performed as we recently described.[9] Briefly, reaction mixtures were spotted on silica plates (Merck) to the desired final concentration. A solvent mixture of *n*-propanol, ammonia, and H_2O was then used in a ratio of 11:2:7 for separating **Rib1P** reactions. Nucleoside and base signals were detected by UV light. **Rib1P** was detected colourimetrically by heating the TLC plates at 110 °C for 5–15 min after treatment with a *p*-anisaldehyde-sulphuric acid solution (*p*-anisaldehyde, concentrated H_2SO_4 and 96% ethanol at a ratio of 1:1:18) *(Figure 12B)*. Inorganic phosphate was detected using the Hanes reagent.[10]

NMR spectroscopy

^{1}H and ^{31}P NMR spectra were recorded in D_2O on a Bruker Avance III 700 MHz or 500 MHz instrument. Chemical shifts are reported in parts per million (ppm) relative to TMS and are referenced to the residual solvent resonance (^{1}H NMR: δ = 2.50 ppm for DMSO-d_5 and δ = 4.79 ppm for HDO).[11] ^{31}P NMR spectra are referenced in compliance with the unified scale relative to H_3PO_4.[12]

For the quantitative determination of impurities, a ^{1}H spectrum with a recycle time between the pulses of 58 s was used to allow full relaxation of the nuclear spins. Two methods were used to determine the integrals: the fitting of the signal shapes with the decon tool of topspin and a careful "normal" integration in topspin.

H,H-NOESY spectra were measured to determine the configuration at the anomeric position. The anomeric alpha configuration of ribose-1-phosphate was concluded from the NOE of hydrogen 1 to hydrogen 3 and a lack of an NOE from hydrogen 1 to hydrogen 4. An authentic sample of Rib1P (BioNukleo GmbH, Berlin, Germany) was used to measure the NOESY. Due to the identical chemical shift, this Rib1P must have the identical anomeric centrum as the products from the enzymatic synthesis developed in this paper.

Greenness evaluation

To evaluate our presented method against other state-of-the-art chemo-enzymatic methods, we followed the recommendation of the CHEM21 zero-pass tool.[13] The tool allows a rapid comparison of different methods by creating categories and assigning flags. Therefore, it is advantageous in the early development of synthesis routes by spotting significant flaws within them. However, we changed the colours to make it more accessible for colour-deficient people.[14] The greenness evaluation part of the supplementary experimental information describes the calculation used for the green metrics.

Finally, we expanded our analysis by the E-factor, which calculates waste production (by dividing the total mass of materials used by the mass of generated product)[15,16] and has proven insightful for comparing nucleoside synthesis routes.[17] For the calculations, we followed a procedure similar to what was recently reported.[17] Briefly, experimental details were taken from the original reports or detailed information was provided: quantities (g, mol) of all starting materials, reaction solvents (L, g), and extraction solvents (L, g), and amount of product (yield, g, mol). Quantities were sorted into the following categories: reagents and organic compounds, inorganics and salts, solvents and water. We calculated the simple E-factor (sEF, considering only reagents and starting materials) and complete E-factor (cEF, further including inorganics, organic solvents, and water) using this raw data. In multistep synthesis routes, the E-factor was extended by the E-factor of the previous steps (by multiplying the mass with the respective E-factor).

If a range of quantities is provided for a given step, we assumed the median value (e.g., if the protocol states 4-6 volumes are needed, we assumed 5). When no data is provided, we assume the values as recommended.[17] All assumed data are marked in *italics* and clearly marked as that. The values were rounded to the nearest plausible gram, with no more than three decimal places.

Supplementary data

Sequences

The added his-tag is marked blue and is encoded on the expression vector.

>*Dg*GuaD (WP_011525960.1, UniProt: Q1J394)

MRGSHHHHHHGSTTGQVTLYRATFMHTPASPFTAPDTLQIQEDGALLVEDGRILAGGPYAQVRA
AQPRAEVVDLRGGVLLPGFIDTHVHYPQVRVLGGLGMGLLEWLDRNTLPEEARLSDPVYARAVA
REFLSALASNGTTTALVFGSHYASAMDVFFEEAARTGLRVVAGQVVSDRLLRPELHTTPERAYAE
GKALIERWHGVGRALYAVTPRFALSASEGILDACGALMRECEGVRFTSHINENPREIETVLQLFPG
ARDYLDPYERAGLVTRRSVLAHNVHPTDRELSVMAAHHCSAAHCPCSNAALGSGLFPLRRHLQA
GVHVSLGTDVGGGTGFSMLKEGLQAYFMQQLLGSAGAVLGPAELLYLATRAGAEALDLQDLTGD
FGVGKAFDAVYLRPPEGTTLATVLRHADSSARVLAALFTLGTGQDVAQVWVGGDSVYRRASSAQ
EVRL

Sequences used for alignment.

>P76641|guanine deaminase|EC 3.5.4.3|*Escherichia coli* (strain K12)|Swiss-Prot|*Ec*GuaD

MMSGEHTLKAVRGSFIDVTRTIDNPEEIASALRFIEDGLLLIKQGKVEWFGEWENGKHQIPDTIRVR
DYRGKLIVPGFVDTHIHYPQSEMVGAYGEQLLEWLNKHTFPTERRYEDLEYAREMSAFFIKQLLRN
GTTTALVFGTVHPQSVDALFEAASHINMRMIAGKVMMDRNAPDYLLDTAESSYHQSKELIERWHK
NGRLLYAITPRFAPTSSPEQMAMAQRLKEEYPDTWVHTHLCENKDEIAWVKSLYPDHDGYLDVYH
QYGLTGKNCVFAHCVHLEEKEWDRLSETKSSIAFCPTSNLYLGSGLFNLKKAWQKKVKVGMGTDI
GAGTTFNMLQTLNEAYKVLQLQGYRLSAYEAFYLATLGGAKSLGLDDLIGNFLPGKEADFVVMEP
TATPLQQLRYDNSVSLVDKLFVMMTLGDDRSIYRTYVDGRLVYERN

>Q07729|guanine deaminase|EC 3.5.4.3|*Saccharomyces cerevisiae* (strain ATCC 204508 / S288c)|Swiss-Prot|*Sc*GuaD
MTKSDLLFDKFNDKHGKFLVFFGTFVDTPKLGELRIREKTSVGVLNGIIRFVNRNSLDPVKDCLDHD
SSLSPEDVTVVDIIGKDKTRNNSFYFPGFVDTHNHVSQYPNVGVFGNSTLLDWLEKYTFPIEAALA
NENIAREVYNKVISKTLSHGTTTVAYYNTIDLKSTKLLAQLSSLLGQRVLVGKVCMDTNGPEYYIED
TKTSFESTVKVVKYIRETICDPLVNPIVTPRFAPSCSRELMQQLSKLVKDENIHVQTHLSENKEEIQ
WVQDLFPECESYTDVYDKYGLLTEKTVLAHCIHLTDAEARVIKQRRCGISHCPISNSSLTSGECRV
RWLLDQGIKVGLGTDVSAGHSCSILTTGRQAFAVSRHLAMRETDHAKLSVSECLFLATMGGAQVL
RMDETLGTFDVGKQFDAQMIDTNAPGSNVDMFHWQLKEKDQMQEQEQEQGQDPYKNPPLLTN
EDIIAKWFFNGDDRNTTKVWVAGQQVYQI

>Q9Y2T3|guanine deaminase|EC 3.5.4.3|*Homo sapiens*|Swiss-Prot|*Hs*GuaD
MCAAQMPPLAHIFRGTFVHSTWTCPMEVLRDHLLGVSDSGKIVFLEEASQQEKLAKEWCFKPCEI
RELSHHEFFMPGLVDTHIHASQYSFAGSSIDLPLLEWLTKYTFPAEHRFQNIDFAEEVYTRVVRRTL
KNGTTTACYFATIHTDSSLLLADITDKFGQRAFVGKVCMDLNDTFPEYKETTEESIKETERFVSEML
QKNYSRVKPIVTPRFSLSCSETLMGELGNIAKTRDLHIQSHISENRDEVEAVKNLYPSYKNYTSVYD
KNNLLTNKTVMAHGCYLSAEELNVFHERGASIAHCPNSNLSLSSGFLNVLEVLKHEVKIGLGTDVA
GGYSYSMLDAIRRAVMVSNILLINKVNEKSLTLKEVFRLATLGGSQALGLDGEIGNFEVGKEFDAILI
NPKASDSPIDLFYGDFFGDISEAVIQKFLYLGDDRNIEEVYVGGKQVVPFSSSV

>2OOD_1|Chain A|Blr3880 protein|*Bradyrhizobium japonicum* (224911)|*Bj*GuaD
MSLTTVGIRGTFFDFVDDPWKHIGNEQAAARFHQDGLMVVTDGVIKAFGPYEKIAAAHPGVEITHI
KDRIIVPGFIDGHIHLPQTRVLGAYGEQLLPWLQKSIYPEEIKYKDRNYAREGVKRFLDALLAAGTTT
CQAFTSSSPVATEELFEEASRRNMRVIAGLTGIDRNAPAEFIDTPENFYRDSKRLIAQYHDKGRNL
YAITPRFAFGASPELLKACQRLKHEHPDCWVNTHISENPAECSGVLVEHPDCQDYLGVYEKFDLV
GPKFSGGHGVYLSNNEFRRMSKKGAAVVFCPCSNLFLGSGLFRLGRATDPEHRVKMSFGTDVG
GGNRFSMISVLDDAYKVGMCNNTLLDGSIDPSRKDLAEAERNKLSPYRGFWSVTLGGAEGLYIDD
KLGNFEPGKEADFVALDPNGGQLAQPWHQSLIADGAGPRTVDEAASMLFAVMMVGDDRCVDET
WVMGKRLYKKSEGHHHHHH

Genome mining and characterisation of a thermostable GuaD

Thermostability is considered one of the most critical factors for applying enzymes in bioindustry.[18,19] As such, most NP-mediated chemistry is with thermostable NPs.[3,4,20,21] Therefore, we re-analysed the genomic space of well-described thermophilic bacteria (*Deinococcus geothermalis, Parageobacillus thermoglucosidasius, Thermus thermophilus and Thermotoga maritima*) for annotated GuaDs. Surprisingly, we only found a guanine deaminase for *D. geothermalis*. Hence, we decided to study both GuaD from *D. geothermalis* and the well-known *E. coli* GuaD. As re-cloning of the *guaD* into the expression plasmid failed for the *E. coli* enzyme, we only proceeded with *Dg*GuaD. We expressed it in *E. coli* BL21 as an N-terminal his-tagged version, allowing the recombinant protein to be efficiently purified (*Figure S2*).

There are two classes of GuaD: i) the cytidine and ii) the amidohydrolase superfamily groups, including *Dg*GuaD. Sequence alignments revealed low amino acid identity to the *E. coli, Bradyrhizobium japonicum, Saccharomyces cerevisiae* and *Homo sapiens* GuaD, with 39%, 38%, 31%, and 31%, respectively (*Figure S3, S4*). Despite sharing low identity, AlphaFold prediction[22,23] shows the highly conserved TIM barrel tertiary structure with high structural similarity to the GuaD from *E. coli* (*Ec*GuaD, 6OHB) (*Figure S1A*).

We were first interested in exploring whether *Dg*GuaD discriminates between **Gua** and **Guo**, as other annotated GuaDs have also been shown to accept **Guo**,[24,25] and this would make the application in our coupled system impossible. Initial reactions with **Gua** and **Guo** revealed that only **Gua** serves as a substrate, with complete conversion of **Gua** to **Xan** (*Figure S1B,* see *Figure S6* for time course experiment). To date, little is known about the structure-specificity relationship of aminohydrolase-like guanine deaminases. However, for the structurally well-characterised NE0047 from *Nitrosomonas europaea,*[26,27] (belonging to the cytidine superfamily), which also strictly accepts **Gua**, it was described that the C-terminal loop controls the substrate specificity. The function of this loop is supposed to slide over the catalytic centre like a lid after ligand binding. This conformational change also limits the size of the possible ligands, disallowing the deamination of the bulkier nucleosides.

Curious if other (modified-)nucleobases would also be accepted, we screened a wide panel of nucleobases (including both pyrimidines and purines), none of which were substrates for *Dg*GuaD (*Figure S7*).

Next, we sought to determine the catalytic activity of *Dg*GuaD. Depending on the pH, kinetic experiments determined a single optimum at pH 6-7 (*Figure S1C*). This is comparable with other described GuaDs with single pH optima between 6.8 and 9.4.[28–30] Notably, with a maximum of more than 1400 U mg^{-1} at pH 6 (*Figure S8*), this is the highest measured specific activity of a GuaD to the best of our knowledge. Since the optimal growth temperature of *D. geothermalis* is between 45 °C and 50 °C,[31] we wanted to explore whether *Dg*GuaD is a thermostable enzyme. After determining

the melting temperature (T_m = 75 °C, *Figure S9*), we further explored the 30–60 °C activity range. Surprisingly, there was no strong dependence of activity on temperature (*Figure S1D*). An explanation might be found in the catalytic mechanism. GuaDs catalyse the deamination in three steps, the activation energies of the last two intermediate steps being in the same order of magnitude.[32] Therefore, the first rate-determining step may change due to the increasing temperature. This change would cause the activity to decrease but would be offset by the increased activity due to the increased temperature.

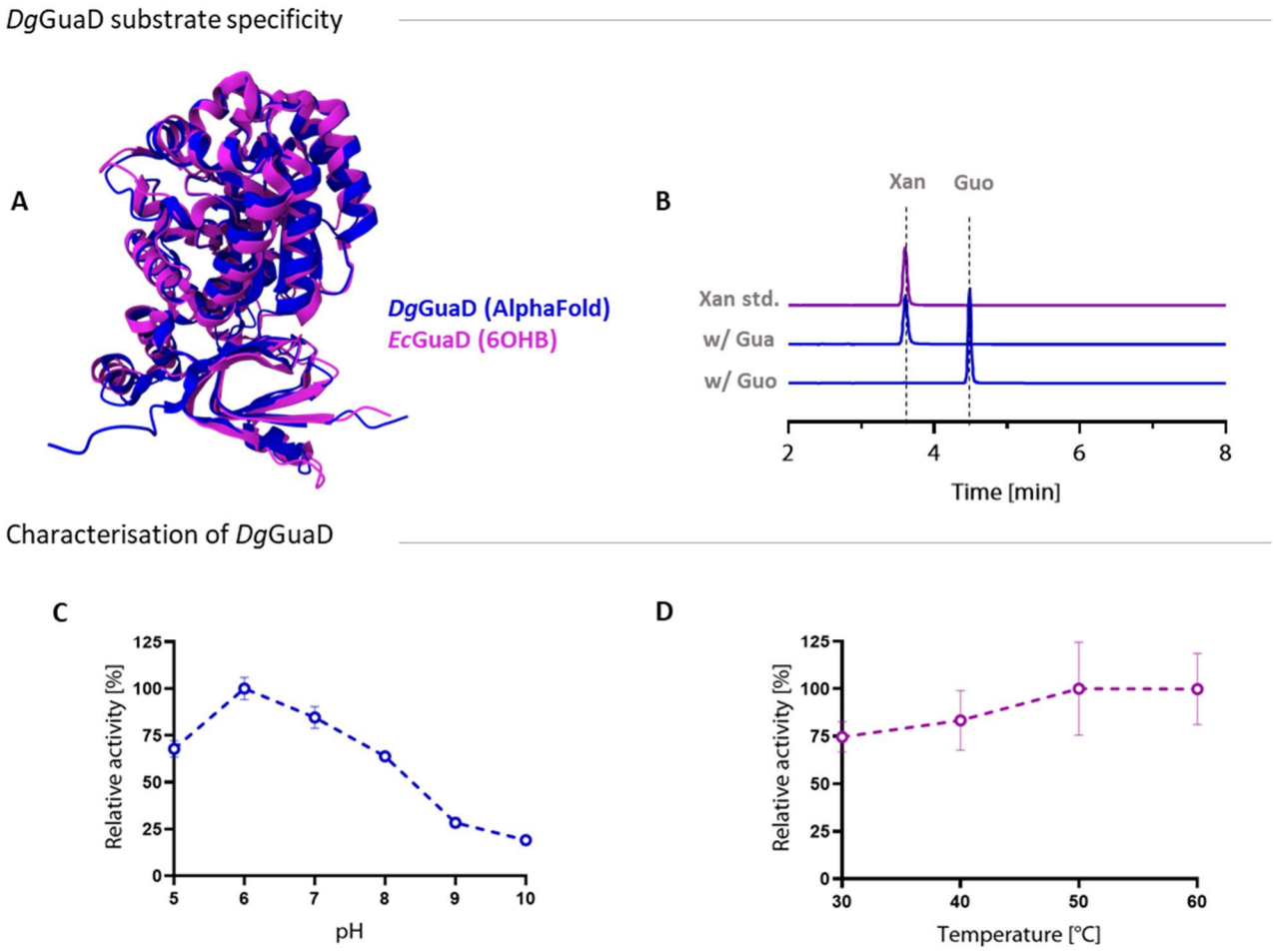

Figure S1. Characterisation of the thermostable *Dg*GuaD. A) Structural alignment of alpha fold prediction of *Dg*GuaD and *Ec*GuaD (PDB id: 6OHB) B) The HPLC traces show reactions employing *Dg*GuaD with Gua or Guo as substrates. The top lane is an authentic Xan standard. C & D) The relative activity of *Dg*GuaD depends on pH and temperature. Measurements were repeated in triplicates. The highest activity was set to 100%.

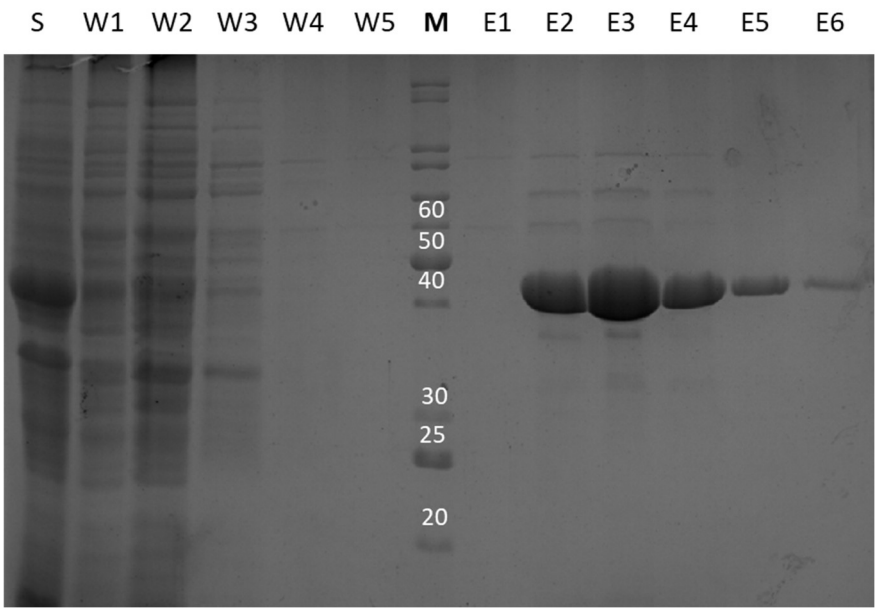

Figure S2. Representative SDS-PAGE of *Dg*GuaD purification**.** S = lysate sample, W = wash fractions, M = marker (kDa), E = elution fraction containing *Dg*GuaD at 40-50 kDa (estimated size is 48 kDa).

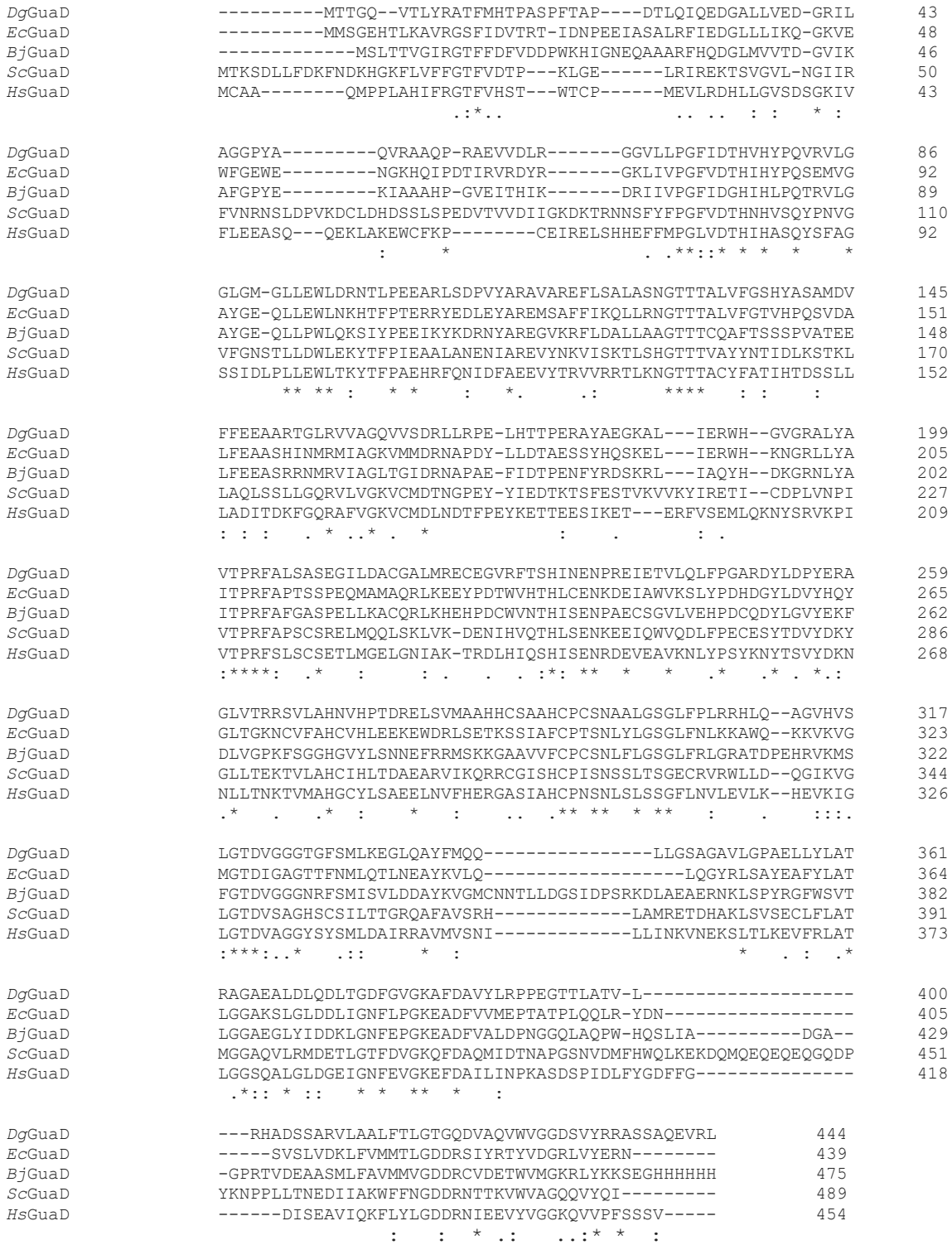

Figure S3. Sequence alignment of well-described GuaDs created by Clustal2.1. GuaD originate from different organisms: *Dg*GuaD = *Deinococcus geothermalis*, *Ec*GuaD = *Escherichia coli*, *Bj*GuaD = *Bradyrhizobium japonicum*, *Sc*GuaD = *Saccharomyces cerevisiae*, *Hs*GuaD = *Homo sapiens*.

1: *Dg*GuaD	100.00	38.84	37.87	31.31	31.34
2: *Ec*GuaD	38.84	100.00	43.22	32.24	34.13
3: *Bj*GuaD	37.87	43.22	100.00	27.95	28.81
4: *Sc*GuaD	31.31	32.24	27.95	100.00	40.13
5: *Hs*GuaD	31.34	34.13	28.81	40.13	100.00

Figure S4. Percent Identity Matrix of the above-shown sequence alignment created by Clustal2.1. *Dg*GuaD = *Deinococcus geothermalis*, *Ec*GuaD = *Escherichia coli*, *Bj*GuaD = *Bradyrhizobium japonicum*, *Sc*GuaD = *Saccharomyces cerevisiae*, *Hs*GuaD = *Homo sapiens*.

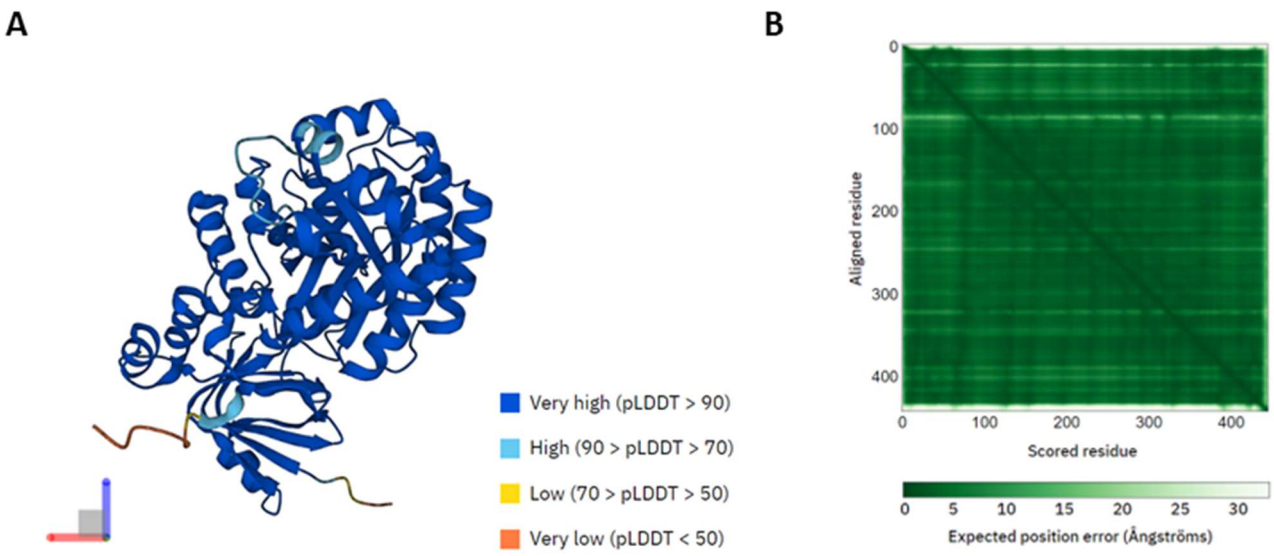

Figure S5. AlphaFold[22,23] prediction of *Dg*GuaD. Accession code is AF-Q1J394-F1**.** This prediction was used for the structural alignment in *Figure S1* and *Table S1*.

Table S1. Structural alignment of *Dg*GuaD AlphaFold prediction (AF-Q1J394-F1) and *Ec*GuaD (6OHB).

Entry	Chain	RMSD	TM-score	Identity	Equivalent Residues	Sequence Length	Modelled Residues
AF-Q1J394-F1	A	-	-	-	-	444	444
6OHB	A	1.58	0.94	38%	431	439	435

Even though they share 38% amino acid identity, the structural alignment shows high structural similarity (RMSD = 1.58 Å). The alignment was performed using the PDB tool (access at https://www.rcsb.org/alignment, jFATCAT (rigid)).

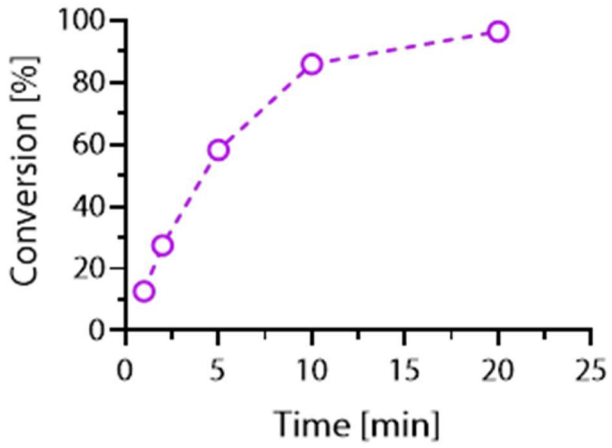

Figure S6. Time course deamination of guanine (Gua) to xanthine (Xan). Reaction conditions were: 40 °C, 50 mM glycine-OH pH 9, 0.2 mM Gua, 0.1 µg mL^{-1} *Dg*GuaD. Samples were analysed via spectral unmixing.

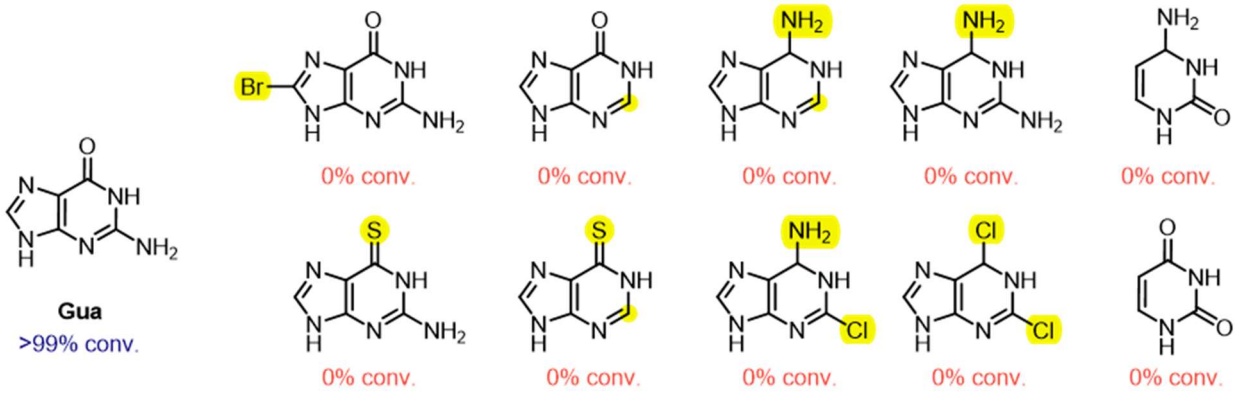

Figure S7. The substrate scope of *Dg*GuaD. Reactions contained 50 mM glycine-OH pH 9, 0.2 mM nucleobase, 1 µg mL^{-1} *Dg*GuaD and were incubated at 40 °C for 20 min. Data was generated by spectral unmixing.

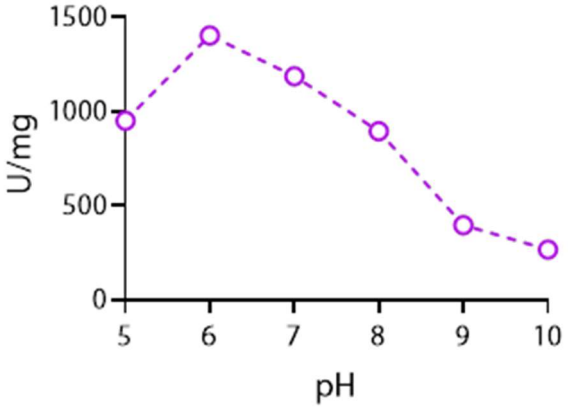

Figure S8. Unnormalised kinetic data in dependence on the pH value. Reactions were performed with 1 mM Gua, 50 mM K_2HPO_4, 50 mM PHB buffer in different pH values, and 10 µL enzyme in a total reaction volume of 500 µL. Reactions were analysed via HPLC. To our knowledge, a specific activity of over 1400 U mg^{-1} for Gua is the highest measured activity compared to other GuaDs.

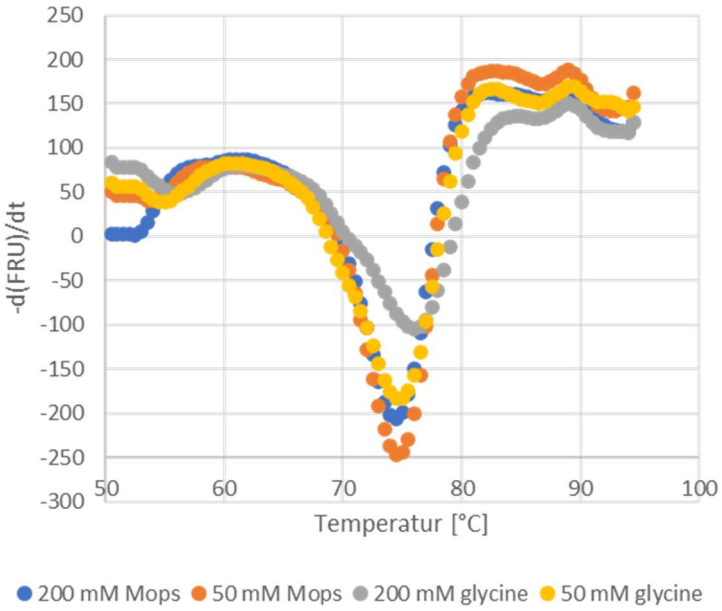

Figure S9. Melting temperature of *Dg*GuaD. Melting temperature was determined in different buffers (MOPS pH 7/glycine-OH pH 9) and concentration (50/200 mM) with 100 µg mL^{-1} *Dg*GuaD.

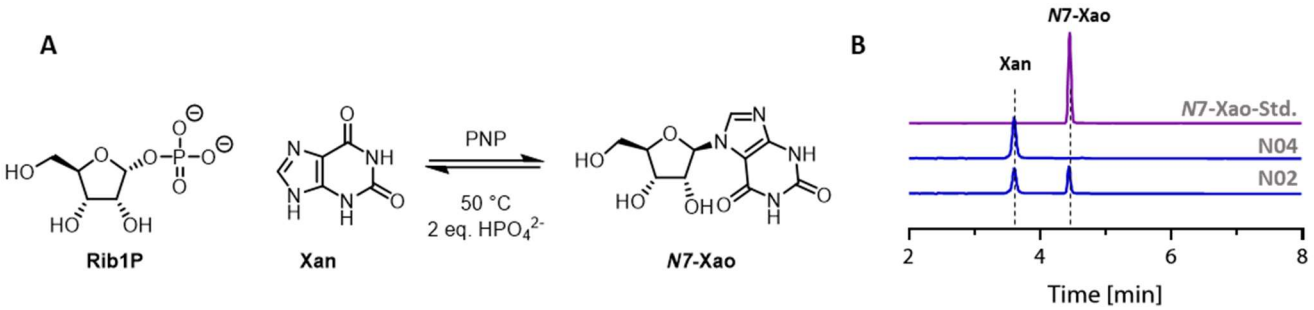

Figure S10. *N7*-xanthosine formation with PNP N02 and PNP N04. A) The reaction conditions contained 50 mM Na-borate buffer pH 9, ~1 mM Xan, 1.25 mM Rib1P, 10 mM phosphate, and 0.075 mg mL^{-1} PNP N02 or PNP N04. The reactions were incubated for 30 min at 50 °C. B) The corresponding HPLC analysis of those reactions. The top lane is an authentic *N7*-Xao standard. Under the given conditions (50°C, excess phosphate and borate buffer) PNP 04 does not produce N7-xanthosine. It was therefore selected for cascade reactions with *Dg*GuaD. The differences between PNP N02 and PNP N04 are probably due to different reaction rates at 50°C: while PNP N02 has an optimum temperature of 50°C, that of PNP N04 is around 80°C.

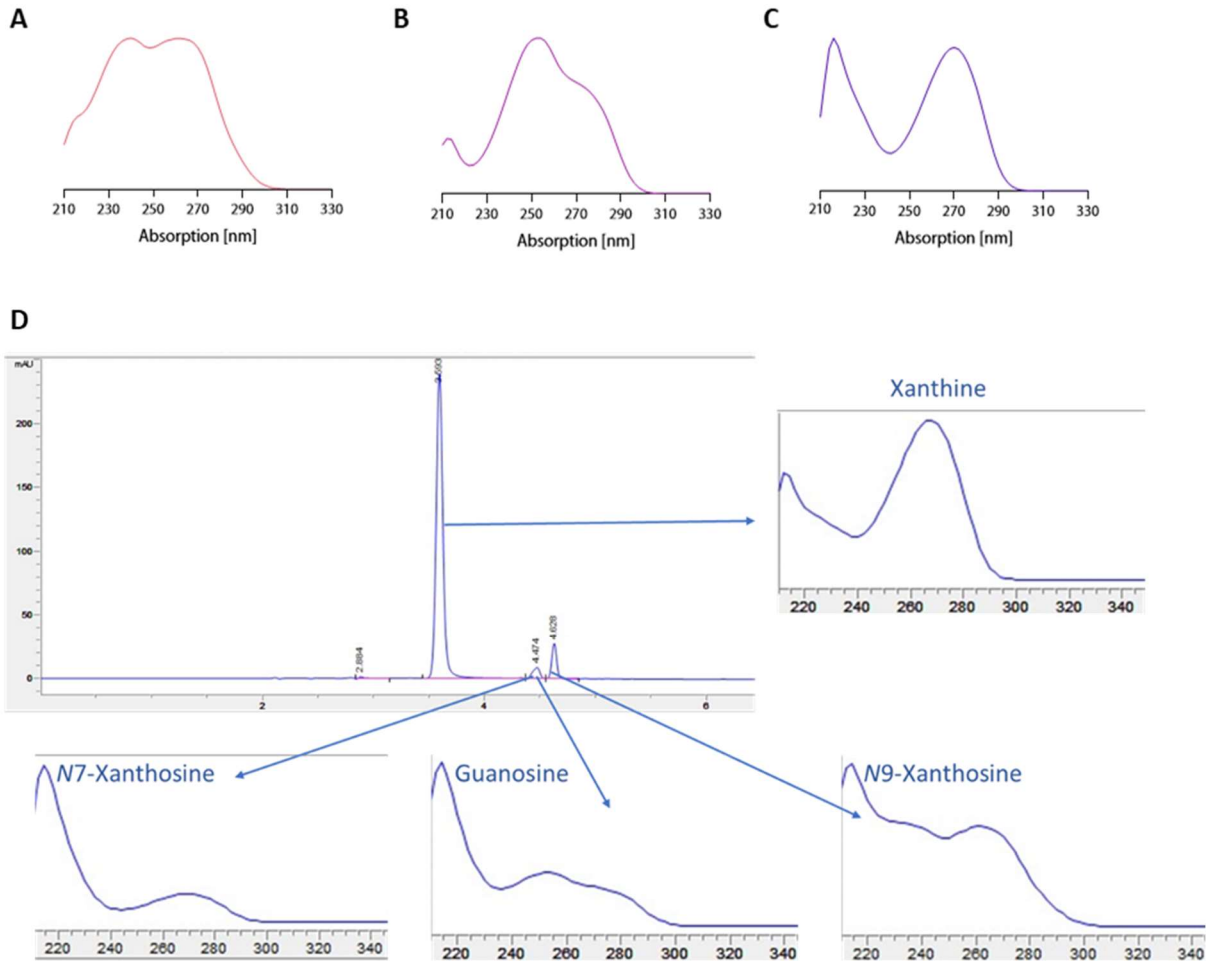

Figure S11. Different UV spectra observed in the biocatalytic cascade reactions. Spectra recorded from an authentic 1 mM standard via HPLC (pH 5). A) *N*9-Xao, B) Guo, C) *N*7-Xao. All these spectra were also detected in the biocatalytic cascades and were used to observe the reaction course. D) Different UV spectra were observed from a representative biocatalytic cascade reaction involving PNP N04. The HPLC chromatogram shows the point of highest conversion to Rib1P before the equilibrium shifts toward Xao formation.

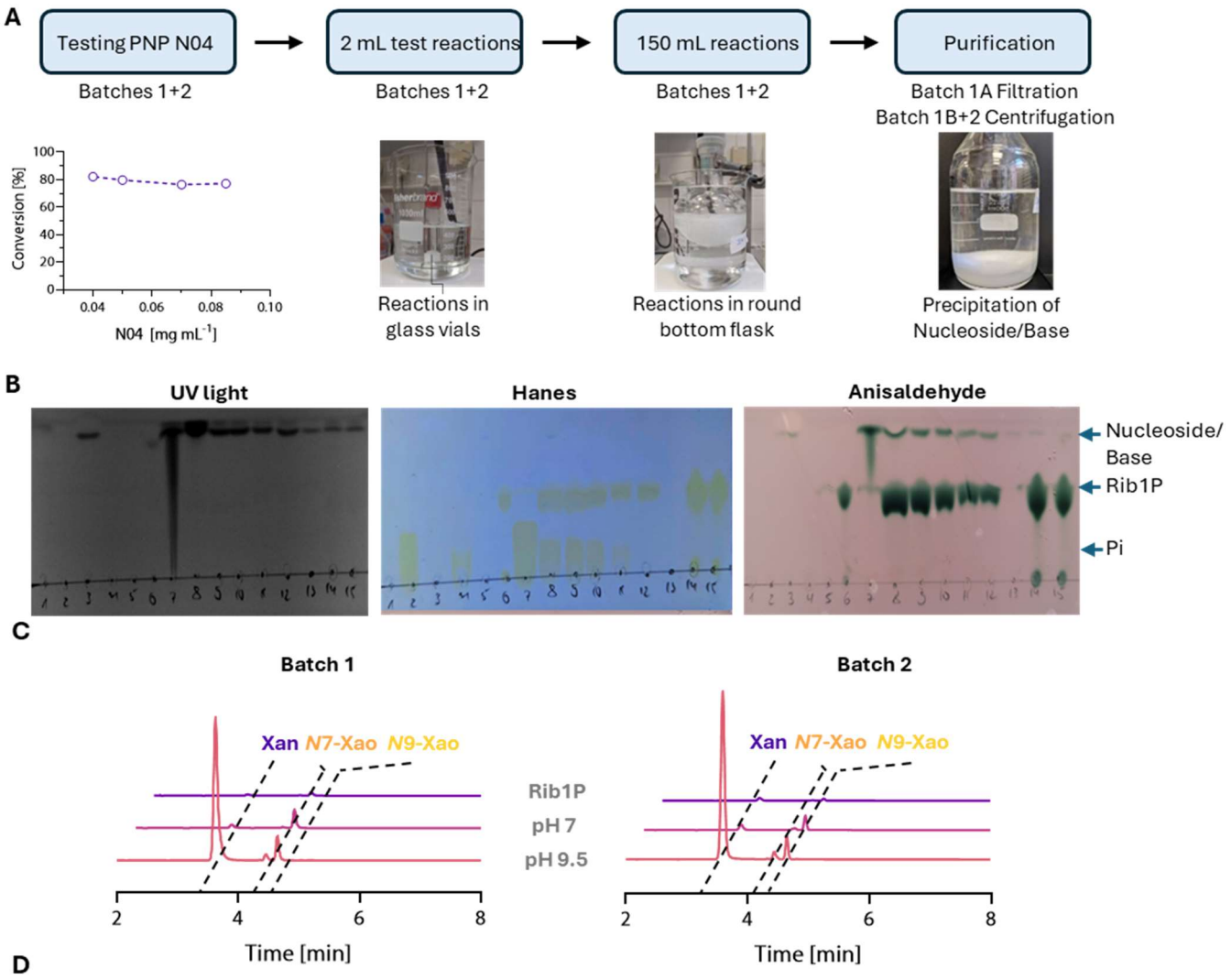

D

Batch	Yield	Rib1P	Acetate	Ethanol	*N*9-Xanthosine	unidentified impurities
1A	65% (0.45 g)	93 ± 1%	3.3 ± 0.4%	2.4 ± 0.3%	0.7 ± 0.2%	< 0.6%
1B	77% (0.53 g)	83 ± 3%	5.2 ± 0.6%	9 ± 1%	1.1 ± 0.3%	< 1.7%
2	79% (1.09 g)	94.4 ± 0.7%	3.8 ± 0.5%	< 0.6%	0.5 ± 0.1%	< 0.7%

Figure S12. Gram-scale synthesis of Rib1P. A) Experimental workflow for the upscaled syntheses. Batch 1 was separated into Batch 1A and Batch 1B to compare filtration and centrifugation. B) Validation of the purification process for batches 1A and 1B by TLC. A: UV light exposure, B: Staining with Hanes reagent, C: Staining with Anisaldehyde solution. 1 = Guo, 2 = K_2HPO_4, 3 = *N*9-Xao, 4 = Xan, 5 = *N*7-Xao, 6 = Rib1P standard, 7 = 150 mL reaction after enzyme addition (t0), 8 = 150 mL reaction after 30 min (t1), 9 = Solution at pH 7, 10 = Solution after nucleoside precipitation, 11 & 12 = phosphate precipitation, 13 = Solution after precipitation as barium salt, 14 = Rib1P after

filtration, 15 = Rib1P after centrifugation. Solvent: *n*-PrOH: NH_3:H_2O = 11:2:7. C) HPLC chromatograms. "pH 9.5" corresponds to the reaction mixture before nucleobase precipitation and "pH 7" afterwards. D) Purity determined by quantitative ^{1}H-NMR measurements. Percentage values are molar ratios of the substances visible in the ^{1}H spectrum.

α-D-ribose-1-phosphate

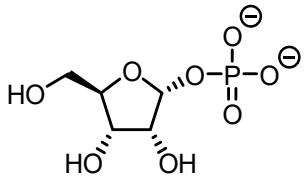

^{1}H NMR (700 MHz, D_2O): δ = 3.73 (dd, ^{2}J = 12.3 Hz, ^{3}J = 5.4 Hz, 1H, H-5A), 3.86 (dd, ^{2}J = 12.4 Hz, ^{3}J = 3.4 Hz, 1H, H-5B), 4.15 (dd, ^{3}J = 6.1 Hz, ^{3}J = 3.9 Hz, 1H, H-3), 4.21 (t, ^{3}J = 4.8 Hz 1H, H-2), 4.31 (mc, 1H, H-4), 5.69 (dd, ^{3}J = 6.4 Hz, ^{3}J = 4.1 Hz, 1H, H-1) ppm. **^{31}P NMR** (202 MHz, D_2O): δ = 2.35 ppm. **HRMS** for $C_5H_{11}O_8P$ calculated $[M+H]^-$: 229.0108, found 229.0108.

For the assignment (2D and NOE) and the coupling information, an authentic **Rib1P** sample (BioNukleo GmbH, Berlin, Germany) was used due to the broad lines in the spectrum of the **Rib1P** obtained from the enzyme cascade (see ^{1}H spectrum). The broad lines are possibly caused by the complexation of the barium ions. The **Rib1P** sample used for the assignment had the same ^{1}H chemical shifts and should therefore contain both **Rib1P**.

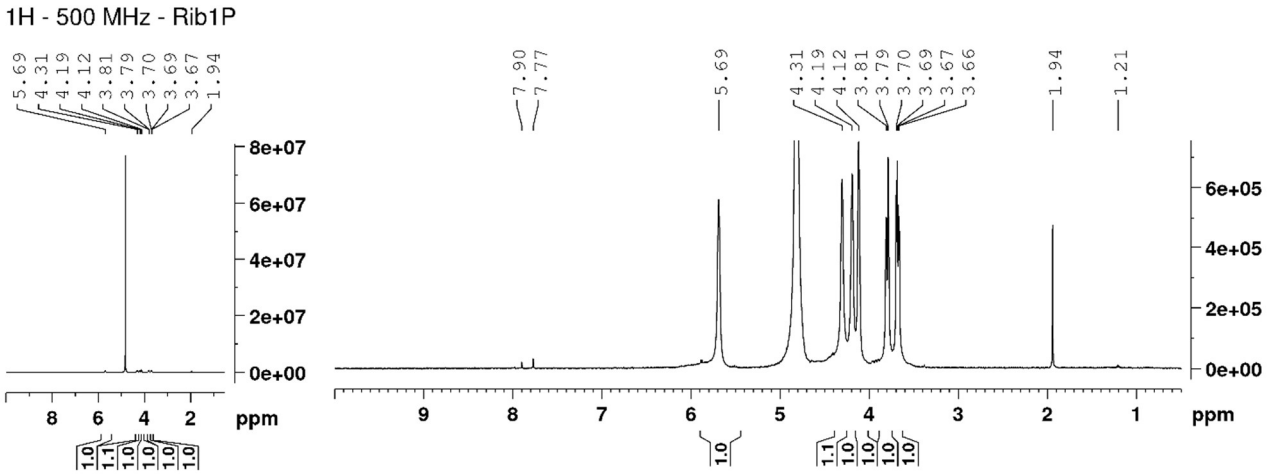

Figure S13. ^{1}H-NMR of Rib1P

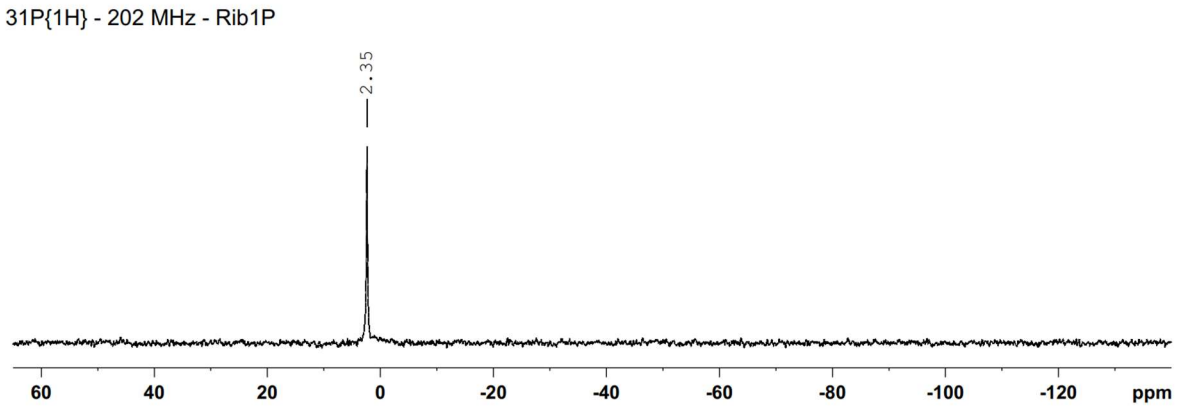

Figure S14. ^{31}P-NMR of Rib1P.

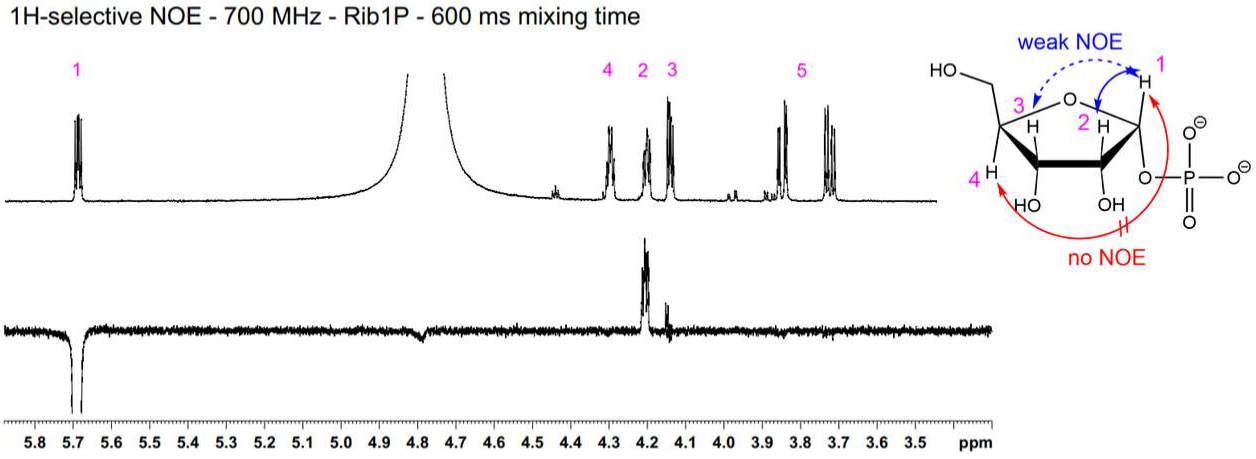

Figure S15. ^{1}H-selective NOESY NMR of Rib1P. The anomeric alpha configuration of ribose-1-phosphate was concluded from the NOE of hydrogen 1 to hydrogen 3 and a lack of an NOE from hydrogen 1 to hydrogen 4.

Green metric calculations

The calculation for Kamel *et al.* (2018)[9]

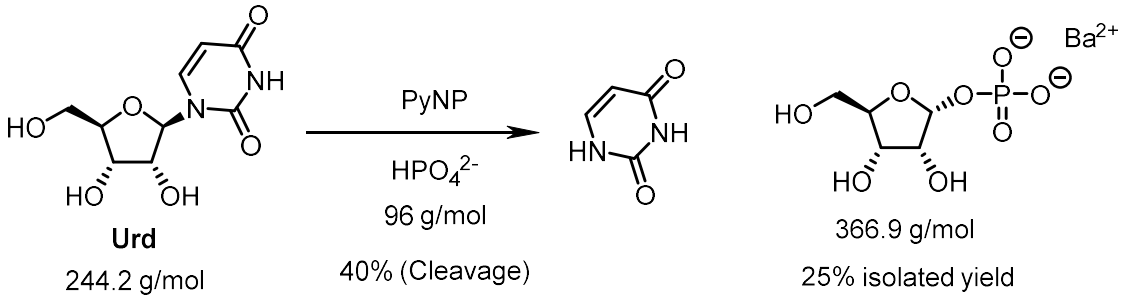

This description is based on the publication by Kamel *et al.* (2018)[9]. However, as the information in the manuscript was not sufficient for the calculation, we used a protocol based on the publication provided by Sarah Kamel. For synthesis, uridine (**14.8 g,** 200 mM, 60.6 mmol) was reacted with the thermostable PyNP Y02 (0.115 mg mL^{-1}, 0.036 g with *3.5 g* water, ρ = 1.00 g cm^{-3}, with an assumed stock concentration of 10 g L^{-1}) with KP puffer (150 mL, 126.5 g with ρ = 1.00 g cm^{-3}, 1 M (500 mM in the final reaction) with potassium phosphate dibasic (MW: 174.18 g mol^{-1} 14 g and potassium phosphate monobasic 9.5 g (MW: 136.09 g mol^{-1})) and water (*146.5 mL*, *146.5 g*, with ρ = 1.00 g cm^{-3}). After 24 h, the reaction was cooled and filtered, and ammonia was added (100 mL 25%, 90.3 g, ρ = 0.903 g cm^{-3}). The remaining free phosphates were precipitated with ammonium chloride and magnesium chloride (81 g NH_4Cl (6 M, MW: 53.491 g mol^{-1}), 31 g $MgCl_2$ (1.3 M, MW: 95.211 g mol^{-1}) in 138 g with ρ = 1.00 g cm^{-3} water). After cooling and filtration, the solution was concentrated to 300 mL, and ammonia was added (30 mL 25%, 27.1 g, ρ = 0.903 g cm^{-3}). **Rib1P** was precipitated with barium acetate (16 g, 1.8 M, MW: 255.415 g mol^{-1} with 34 g water, ρ = 1.00 g cm^{-3}) and ethanol (600 mL, 481.8 g with ρ = 0.803 g cm^{-3}) for 24 h at 4 °C. Finally, **Rib1P** salts were collected by centrifugation in centrifugation tubes (we assumed 6 tubes) and washed three times in ethanol (25 mL * 6 (tubes) * 3 = 450 mL, *357.3 g* with ρ = 0.794 g cm^{-3}) before drying at 40 °C provided **5.5 g** product (25% yield, 15 mmol).

E-Factor calculations

Thus, the preparation of **Rib1P** by Kamel *et al.* had a **sEF of 8.9**, calculated as

$$\mathrm{sEF} = \frac{14.8 + 0.036 + 14 + 9.5 + 16 - 5.5}{5.5}$$

and a **cEF of 285** calculated as

$$\mathrm{cEF} = \frac{14.8 + 0.036 + 3.5 + 126.5 + 14 + 9.5 + 146.5 + 90.3 + 81 + 31 + 138 + 27.1 + 16 + 34 + 481.8 + 357.3 - 5.5}{5.5}$$

with contributions from reagents (9.6), inorganics (20.1), organic solvents (173.6) and water (81.3).

CHEM21 Zero Pass calculations

Selectivity was calculated as,

$$Selectivity = \frac{Yield}{Conversion} * 100$$

$$Selectivity = \frac{25}{40} * 100 = \ 63\%$$

and atom economy (AE) as

$$Atom\ economy\ (AE) = \frac{molecular\ weight\ of\ product}{molecular\ weight\ of\ reactants} * 100$$

$$AE = \frac{366.9\ (\mathrm{Rip1P})}{96\ (\mathrm{Phosphate}) + 244.2\ (\mathrm{Urd}) + 137.3\ (\mathrm{Barium})} * 100 = 77\%$$

resulting in **63% selectivity** and **77% atom economy** for the method.

The calculation for Fateev *et al.* (2015)[33]

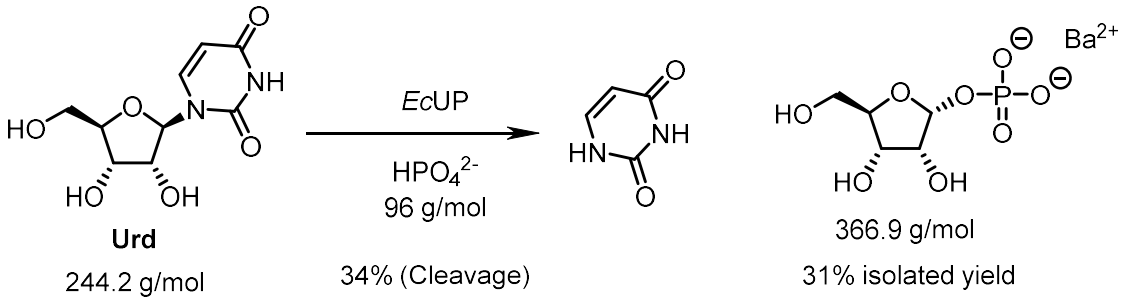

This protocol is based on the publication by Fateev *et al.* (2015).[33] Uridine (**4 g**, 16.4 mmol) was dissolved in a 0.1 M potassium phosphate buffer (330 mL, pH 7.0, thus we assume potassium phosphate dibasic (MW: 174.18 g mol^{-1} *3.1 g* and potassium phosphate monobasic *2.1 g* (MW: 136.09 g mol^{-1})) and water (*324.8 mL*, *324.8 g*, with ρ = 1.00 g cm^{-3}) and reacted with *Ec*UP (25 µL, 56 U, *0.001 g, in 0.024 g* water with ρ = 1.00 g cm^{-3}). The reaction mixture was incubated at 50°C for three days and then cooled to room temperature before the precipitated uracil was filtered off. To the filtrate, a concentrated ammonia solution (25%, 110 mL, 99.3 g, ρ = 0.903 g cm^{-3}) was added, followed by a solution containing ammonium chloride (17.5 g, 325 mmol, 25 M, MW: 53.491 g mol^{-1}) and magnesium chloride decahydrate (10.1 g, 36.7 mmol, 2.9 M, MW: 275.36 g mol^{-1}) in 80 mL water (52.4 g, with ρ = 1.00 g cm^{-3}). This mixture was stored at 4°C overnight and subsequently filtered. The filtrate was evaporated to a volume of 300 mL, then concentrated ammonia (30 mL, we assume 25%, 27.1 g, ρ = 0.903 g cm^{-3}), an aqueous solution of barium acetate (20 mL, 4.3 g, 16.8 mmol, 0.3 M, MW: 255.415 g mol^{-1} with 15.7 g water, ρ = 1.00 g cm^{-3}), and ethanol (300 mL, we assume *240.9 g* with ρ = 0.803 g cm^{-3}) was added. After standing for one day at 4 °C, the precipitated **Rib1P** (barium salt) was filtered off, washed with ethanol (amount not stated; we thus assume an equal amount to the before filtered solution, 350 mL with *261.1 g*, ρ = 0.803 g cm^{-3}) and dried under vacuum over P_2O_5. Yield: **1.86 g** (5.1 mmol, 31%).

E-Factor calculations

Thus, the preparation of **Rib1P** by Fateev *et al.* had a **sEF of 5.1**, calculated as

$$\mathrm{sEF} = \frac{4 + 3.1 + 2.1 + 0.0006 + 4.3 - 1.86}{1.86}$$

and a **cEF of 570** calculated as

$$\mathrm{cEF} = \frac{4 + 3.1 + 2.1 + 324.8 + 0.001 + 0.024 + 99.3 + 17.5 + 10.1 + 52.4 + 27.1 + 4.3 + 15.7 + 240.9 + 261.1 - 1.86}{1.86}$$

with contributions from reagents (7), inorganics (14.6), organic solvents (337.6) and water (211).

CHEM21 Zero Pass calculations

Selectivity was calculated as,

$$Selectivity = \frac{31}{34} * 100 = \ 92\%$$

and AE as

$$AE = \frac{366.9\ (\mathrm{Rip1P})}{96\ (\mathrm{Phosphate}) + 244.2\ (\mathrm{Urd}) + 137.3\ (\mathrm{Barium})} * 100 = 77\%$$

resulting in **92% selectivity** and **77% atom economy** for the method.

The calculation for the method presented in Kulikova *et al.* 2019[34] and Varizhuk et al.[35]

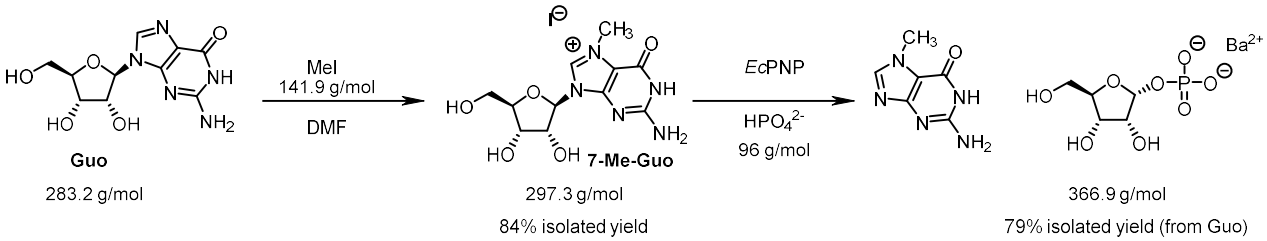

This method is based on Kulikova *et al.* 2019[34]. However, the group posted a follow-up paper 2022[35] providing a step-by-step protocol for the synthesis on which this calculation is performed. Guanosine dihydrate (**5 g**, 15.6 mmol) was reacted with iodomethane (4.4 mL, 10.03 g with ρ = 2.28 g cm^{-3}, 70.5 mmol) in DMF (100 mL, 95 g with ρ = 0.95 g cm^{-3}) for 25 h. The mixture was filtered and washed twice with 10 mL DMF (20 mL, 19 g with ρ = 0.95 g cm^{-3}) before adding CH_2Cl_2 (1.1 L, 1463 g with ρ = 1.33 g cm^{-3}) to precipitate the methylated nucleoside over 16 h. The precipitate was filtered off, washed with diethyl ether (50 mL, 35.5 g with ρ = 0.71 g cm^{-3}) and CH_2Cl_2 (100 mL, 133 g with ρ = 1.33 g cm^{-3}) and dried for 1 h to provide pure 7-methylguanosine hydroiodide in 84% yield (**5.6 g**). Preparation of **Rib1P** was subsequently performed with 200 mg methylguanosine hydroiodide. Therefore, 7-methylguanosine (0.2 g, 0.47 mmol) dissolved in Tris-HCl buffer (90 mL, 50 mM, 0.71 g with MW: 121.14 g mol^{-1} and 89.3 g water with ρ = 1.00 g cm^{-3}) and was reacted with 2 U *Ec*PNP (commercially available from Merck, has an activity of 10 U per mg protein typically, we thus assume *0.002 g*) and potassium phosphate buffer solution (9.9 mL, 50 mM, pH 7.5, with 0.064 g potassium phosphate dibasic (MW: 174.18 g mol^{-1}) and 0.018 g potassium phosphate monobasic (MW: 136.09 g mol^{-1}) and 9.8 g water, with ρ = 1.00 g cm^{-3}) for 6 h. The reaction mixture was filtered, and the aqueous layer was extracted twice with *n*-butanol (200 mL, 162 g, with ρ = 0.81 g cm^{-3}). 0.126 g barium acetate was dissolved in water (2 mL, 2 g, ρ = 1.00 g cm^{-3}) and 0.9 mL ammonia (25%, 0.82 g with ρ = 0.903 g cm^{-3}) and added to the extracted layer overnight. After filtration, the reaction was concentrated to 20 mL. EtOH was added (4−6 volumes are mentioned in the protocol. Thus, we assumed 5 = 100 mL EtOH, *80.3 g* with ρ = 0.803 g cm^{-3}) and incubated overnight at 4 °C. Precipitants were collected by centrifugation (we here assume 6 * 50 mL tubes) and washed with EtOH (6 * 5 mL, 30 mL, *24.1 g* with ρ = 0.803 g cm^{-3}) and diethyl ether (6 * 5 mL, 30 mL, *21.4 g* with ρ = 0.713 g cm^{-3}) before drying under vacuum yielded **0.161 g** (94% from 7-methylguanosine and 79% from guanosine (0.94 * 0.84), 0.44 mmol).

E-Factor calculations

Thus, the preparation of **Rib1P** had **sEF of 3.7** considering the sEF of the starting material 7-methylguanosine as 1.7, calculated as

$$\text{sEF}\ (7-\text{methylguanosine}) = \frac{5 + 10.03 - 5.6}{5.6}$$

$$\text{sEF}\ (\text{Rib1P}) = \frac{0.2 + 0.2 * 1.7 + 0.002 + 0.064 + 0.018 + 0.126 - 0.161}{0.161}$$

and a **cEF of 2816,** considering the cEF of 7-methylguanosine as 313.4 calculated as

$$\text{cEF}\ (7-\text{methylguanosine}) = \frac{5 + 10.03 + 95 + 19 + 1463 + 35.5 + 133 - 5.6}{5.6}$$

$$\text{cEF}\ (\text{Rib1P}) = \frac{\begin{matrix}0.2 + 0.2 * 313.4 + 0.002 + 0.71 + 89.3 + 0.064 + 0.018 + 9.8 + 162 + 0.126 \\ 2 + 0.82 + 80.3 + 24.1 + 21.4 - 0.161\end{matrix}}{0.161}$$

with contributions from reagents (391.6), inorganics (4.2), organic solvents (1792.4) and water (627.7).

CHEM21 Zero Pass calculations

Selectivity was calculated as,

$$Selectivity = \frac{79}{99} * 100 = 80\%$$

considering the total yield from guanosine as 79% and the conversion as 99% (100% conversion in the first synthesis step and 99% in the second),

and AE for the multistep synthesis as,

$$AE = \frac{366.9\ (\text{Rip1P})}{141.9\ (\text{Mel}) + 283.2\ (\text{Guo}) + 96\ (\text{Phosphate}) + 137.3\ (\text{Barium})} * 100 = 56\%$$

resulting in **79% selectivity** and **56% atom economy** for the presented method.

The calculation for the method presented in this paper

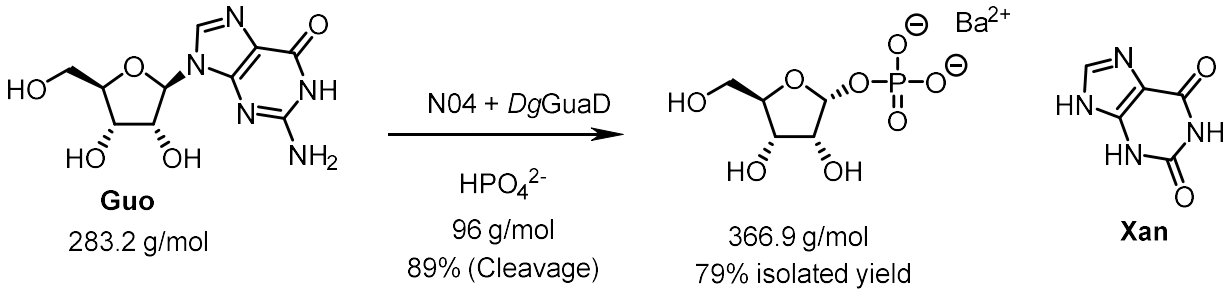

The method is described already in the experimental section. Specific concentrations were taken from the second synthesis and purification run. Guanosine (**1.06 g**, 25 mM, 3.74 mmol) was reacted with K_2HPO_4 (30 mM, 0.024 g in 4476.6 mL, 4.48 g water ρ = 1.00 g cm^{-3}) enzymes PNP N04 (final conc. 0.04 mg mL^{-1}, 0.006 g with 8.82 g water (ρ = 1.00 g cm^{-3}) from an 0.68 mg mL^{-1} stock concentration) and *Dg*GuaD (final conc. 0.016 mg mL^{-1}, 0.002 g with 1.41 g water from a 1.7 mg mL^{-1} stock concentration, with ρ = 1.00 g cm^{-3}) in a total volume of 150 mL (135.3 g water, ρ = 1.00 g cm^{-3}) for 35 min at 50 °C. After freeze-thawing, the reaction mixture was filtered and buffered to pH 7 (a few drops conc. HCl) to precipitate free nucleobases and nucleosides at 4 °C. Ammonia was added (50 mL, 25%, 45.2 g with ρ = 0.903 g cm^{-3}), and phosphates were precipitated with a solution of $MgCl_2$ (0.37 g $MgCl_2$ (31.1 mM, MW: 95.211 g mol^{-1}), and NH_4Cl (0.096 g, 14.5 mM, MW: 53.491 g mol^{-1}) in 124.5 g water, ρ = 1.00 g cm^{-3}). The solution was incubated overnight (16 h) and filtered. The filtrate was used directly for barium precipitation with barium acetate (1 g, 78.3 mM, MW: 255.415 g mol^{-1}) with 49 g water, ρ = 1.00 g cm^{-3}), followed by ethanol addition (600 mL, 481.8 g with ρ = 0.803 g cm^{-3}). The barium salts of **Rib1P** were precipitated at 4 °C overnight (16-20 h). The precipitated salts were collected by centrifugation and were washed 2−3 times with absolute ethanol (>99.8%, 6 tubes, a total of 90 mL (6 * 3 * 5 (mL per wash step)), 71.2 g, with ρ = 0.791 g cm^{-3}) and dried at 50 °C. The protocol yielded **1.09 g** (79%, 2.97 mmol) isolated yield.

E-Factor calculations

Thus, the preparation of Rib1P had a **sEF of 0.9**, calculated as

$$\mathrm{sEF} = \frac{1.06 + 0.024 + 0.006 + 0.002 + 1 - 1.09}{1.09}$$

and a **cEF of 847** calculated as

$$\mathrm{cEF} = \frac{1.06 + 0.024 + 4.48 + 0.006 + 8.82 + 0.002 + 1.41 + 135.3 + 45.2 + 0.37 + 0.096 + 124.5 + 1 + 49 + 481.8 + 71.2 - 1.09}{1.09}$$

with contributions from reagents (1.6), inorganics (0.2), organic solvents (548.5) and water (296.5).

CHEM21 Zero Pass calculations

Selectivity was calculated as,

$$Selectivity = \frac{79}{88} * 100 = 90\%$$

and AE as,

$$AE = \frac{366.9\ (\mathrm{Rib1P})}{96\ (\mathrm{Phosphate}) + 283.2\ (\mathrm{Guo}) + 137.3\ (\mathrm{Barium})} * 100 = 71\%$$

resulting in **90% selectivity** and **71% atom economy** for the presented method.

References

(1) Motter, J. Data for “A Deamination-Driven Biocatalytic Cascade for the Synthesis of Ribose-1-Phosphate,” **2024**. https://doi.org/10.5281/zenodo.10604602.

(2) Zhou, X. Thermostable Nucleoside Phosphorylases as Biocatalysts for the Synthesis of Purine Nucleoside Analogues, **2014**. https://depositonce.tu-berlin.de/items/urn:nbn:de:kobv:83-opus4-51201 (accessed 2024-09-10).

(3) Winkler, K. F.; Panse, L.; Maiwald, C.; Hayeß, J.; Fischer, P.; Fehlau, M.; Neubauer, P.; Kurreck, A. Screening the Thermotoga Maritima Genome for New Wide-Spectrum Nucleoside and Nucleotide Kinases. *Journal of Biological Chemistry* **2023**, *299* (6). https://doi.org/10.1016/j.jbc.2023.104746.

(4) Westarp, S.; Benckendorff, C.; Motter, J.; Rohrs, V.; Sanghvi, Y.; Neubauer, P.; Kurreck, J.; Kurreck, A.; Miller, G. J. Biocatalytic Nucleobase Diversification of 4’-Thionucleosides and Application of Derived 5-Ethynyl-4’-Thiouridine for RNA Synthesis Detection. *Angewandte Chemie International Edition n/a* (n/a), e202405040. https://doi.org/10.1002/anie.202405040.

(5) Kaspar, F.; Giessmann, R. T.; Neubauer, P.; Wagner, A.; Gimpel, M. Thermodynamic Reaction Control of Nucleoside Phosphorolysis. *Advanced Synthesis & Catalysis* **2020**, *362* (4), 867–876. https://doi.org/10.1002/adsc.201901230.

(6) Kaspar, F.; Giessmann, R. T.; Westarp, S.; Hellendahl, K. F.; Krausch, N.; Thiele, I.; Walczak, M. C.; Neubauer, P.; Wagner, A. Spectral Unmixing-Based Reaction Monitoring of Transformations between Nucleosides and Nucleobases. *ChemBioChem* **2020**, *21* (18), 2604–2610. https://doi.org/10.1002/cbic.202000204.

(7) Kaspar, F.; Giessmann, R. T.; Krausch, N.; Neubauer, P.; Wagner, A.; Gimpel, M. A UV/Vis Spectroscopy-Based Assay for Monitoring of Transformations Between Nucleosides and Nucleobases. *Methods and Protocols* **2019**, *2* (3), 60. https://doi.org/10.3390/mps2030060.

(8) Westarp, S.; Brandt, F.; Neumair, L.; Betz, C.; Dagane, A.; Kemper, S.; Jacob, C. R.; Neubauer, P.; Kurreck, A.; Kaspar, F. Nucleoside Phosphorylases Make N7-Xanthosine. *Nat Commun* **2024**, *15* (1), 3625. https://doi.org/10.1038/s41467-024-47287-4.

(9) Kamel, S.; Weiß, M.; Klare, H. F. T.; Mikhailopulo, I. A.; Neubauer, P.; Wagner, A. Chemo-Enzymatic Synthesis of α-d-Pentofuranose-1-Phosphates Using Thermostable Pyrimidine Nucleoside Phosphorylases. *Molecular Catalysis* **2018**, *458*, 52–59. https://doi.org/10.1016/j.mcat.2018.07.028.

(10) Stanley, C. W. Thin-Layer Chromatography of Organophosphorus Pesticides and Acids on Microchromatoplates. *Journal of Chromatography A* **1964**, *16*, 467–475. https://doi.org/10.1016/S0021-9673(01)82517-6.

(11) Fulmer, G. R.; Miller, A. J. M.; Sherden, N. H.; Gottlieb, H. E.; Nudelman, A.; Stoltz, B. M.; Bercaw, J. E.; Goldberg, K. I. NMR Chemical Shifts of Trace Impurities: Common Laboratory Solvents, Organics, and Gases in Deuterated Solvents Relevant to the Organometallic Chemist. *Organometallics* **2010**, *29* (9), 2176–2179. https://doi.org/10.1021/om100106e.

(12) Harris, R. K.; Becker, E. D.; Menezes, S. M. C. de; Goodfellow, R.; Granger, P. NMR Nomenclature. Nuclear Spin Properties and Conventions for Chemical Shifts(IUPAC Recommendations 2001). *Pure and Applied Chemistry* **2001**, *73* (11), 1795–1818. https://doi.org/10.1351/pac200173111795.

(13) McElroy, C. R.; Constantinou, A.; Jones, L. C.; Summerton, L.; Clark, J. H. Towards a Holistic Approach to Metrics for the 21st Century Pharmaceutical Industry. *Green Chem.* **2015**, *17* (5), 3111–3121. https://doi.org/10.1039/C5GC00340G.

(14) Kaspar, F.; Crameri, F. Coloring Chemistry—How Mindful Color Choices Improve Chemical Communication. *Angewandte Chemie International Edition* **2022**, *61* (16), e202114910. https://doi.org/10.1002/anie.202114910.

(15) A. Sheldon, R. The E Factor 25 Years on: The Rise of Green Chemistry and Sustainability. *Green Chemistry* **2017**, *19* (1), 18–43. https://doi.org/10.1039/C6GC02157C.

(16) A. Sheldon, R. The E Factor: Fifteen Years On. *Green Chemistry* **2007**, *9* (12), 1273–1283. https://doi.org/10.1039/B713736M.

(17) Kaspar, F.; Stone, M. R. L.; Neubauer, P.; Kurreck, A. Route Efficiency Assessment and Review of the Synthesis of β-Nucleosides via N-Glycosylation of Nucleobases. *Green Chem.* **2021**, *23* (1), 37–50. https://doi.org/10.1039/D0GC02665D.
(18) Peccati, F.; Alunno-Rufini, S.; Jiménez-Osés, G. Accurate Prediction of Enzyme Thermostabilization with Rosetta Using AlphaFold Ensembles. *J. Chem. Inf. Model.* **2023**, *63* (3), 898–909. https://doi.org/10.1021/acs.jcim.2c01083.
(19) Kunka, A.; Marques, S. M.; Havlasek, M.; Vasina, M.; Velatova, N.; Cengelova, L.; Kovar, D.; Damborsky, J.; Marek, M.; Bednar, D.; Prokop, Z. Advancing Enzyme's Stability and Catalytic Efficiency through Synergy of Force-Field Calculations, Evolutionary Analysis, and Machine Learning. *ACS Catal.* **2023**, *13* (19), 12506–12518. https://doi.org/10.1021/acscatal.3c02575.
(20) Kaspar, F.; Seeger, M.; Westarp, S.; Köllmann, C.; Lehmann, A. P.; Pausch, P.; Kemper, S.; Neubauer, P.; Bange, G.; Schallmey, A.; Werz, D. B.; Kurreck, A. Diversification of 4′-Methylated Nucleosides by Nucleoside Phosphorylases. *ACS Catal.* **2021**, *11* (17), 10830–10835. https://doi.org/10.1021/acscatal.1c02589.
(21) Kaspar, F.; Brandt, F.; Westarp, S.; Eilert, L.; Kemper, S.; Kurreck, A.; Neubauer, P.; Jacob, C. R.; Schallmey, A. Biased Borate Esterification during Nucleoside Phosphorylase-Catalyzed Reactions: Apparent Equilibrium Shifts and Kinetic Implications**. *Angewandte Chemie International Edition* **2023**, *62* (20), e202218492. https://doi.org/10.1002/anie.202218492.
(22) Jumper, J.; Evans, R.; Pritzel, A.; Green, T.; Figurnov, M.; Ronneberger, O.; Tunyasuvunakool, K.; Bates, R.; Žídek, A.; Potapenko, A.; Bridgland, A.; Meyer, C.; Kohl, S. A. A.; Ballard, A. J.; Cowie, A.; Romera-Paredes, B.; Nikolov, S.; Jain, R.; Adler, J.; Back, T.; Petersen, S.; Reiman, D.; Clancy, E.; Zielinski, M.; Steinegger, M.; Pacholska, M.; Berghammer, T.; Bodenstein, S.; Silver, D.; Vinyals, O.; Senior, A. W.; Kavukcuoglu, K.; Kohli, P.; Hassabis, D. Highly Accurate Protein Structure Prediction with AlphaFold. *Nature* **2021**, *596* (7873), 583–589. https://doi.org/10.1038/s41586-021-03819-2.
(23) Varadi, M.; Anyango, S.; Deshpande, M.; Nair, S.; Natassia, C.; Yordanova, G.; Yuan, D.; Stroe, O.; Wood, G.; Laydon, A.; Žídek, A.; Green, T.; Tunyasuvunakool, K.; Petersen, S.; Jumper, J.; Clancy, E.; Green, R.; Vora, A.; Lutfi, M.; Figurnov, M.; Cowie, A.; Hobbs, N.; Kohli, P.; Kleywegt, G.; Birney, E.; Hassabis, D.; Velankar, S. AlphaFold Protein Structure Database: Massively Expanding the Structural Coverage of Protein-Sequence Space with High-Accuracy Models. *Nucleic Acids Research* **2022**, *50* (D1), D439–D444. https://doi.org/10.1093/nar/gkab1061.
(24) Trautwein-Schult, A.; Jankowska, D.; Cordes, A.; Hoferichter, P.; Klein, C.; Matros, A.; Mock, H.-P.; Baronian, K.; Bode, R.; Kunze, G. Arxula Adeninivorans Recombinant Guanine Deaminase and Its Application in the Production of Food with Low Purine Content. *Journal of Molecular Microbiology and Biotechnology* **2014**, *24* (2), 67–81. https://doi.org/10.1159/000357674.
(25) Kim, J.; Park, S. I.; Ahn, C.; Kim, H.; Yim, J. Guanine Deaminase Functions as Dihydropterin Deaminase in the Biosynthesis of Aurodrosopterin, a Minor Red Eye Pigment of Drosophila. *J Biol Chem* **2009**, *284* (35), 23426–23435. https://doi.org/10.1074/jbc.M109.016493.
(26) Bitra, A.; Biswas, A.; Anand, R. *Structural Basis of the Substrate Specificity of Cytidine Deaminase Superfamily Guanine Deaminase*. ACS Publications. https://doi.org/10.1021/bi400818e.
(27) Bitra, A.; Hussain, B.; Tanwar, A. S.; Anand, R. Identification of Function and Mechanistic Insights of Guanine Deaminase from Nitrosomonas Europaea: Role of the C-Terminal Loop in Catalysis. *Biochemistry* **2013**, *52* (20), 3512–3522. https://doi.org/10.1021/bi400068g.
(28) Gupta, N. K.; Glantz, M. D. Isolation and Characterization of Human Liver Guanine Deaminase. *Archives of Biochemistry and Biophysics* **1985**, *236* (1), 266–276. https://doi.org/10.1016/0003-9861(85)90626-5.
(29) Bergstrom, J. D.; Bieber, A. L. Characterization of Purified Guanine Aminohydrolase. *Archives of Biochemistry and Biophysics* **1979**, *194* (1), 107–116. https://doi.org/10.1016/0003-9861(79)90600-3.
(30) Nolan, L. L. Partial Purification and Characterization of Guanine Aminohydrolase Fromtrypanosoma Cruzi. *Current Microbiology* **1984**, *11* (4), 217–220. https://doi.org/10.1007/BF01567163.

(31) Ferreira, A. C.; Nobre, M. F.; Rainey, F. A.; Silva, M. T.; Wait, R.; Burghardt, J.; Chung, A. P.; Da Costa, M. S. Deinococcus Geothermalis Sp. Nov. and Deinococcus Murrayi Sp. Nov., Two Extremely Radiation-Resistant and Slightly Thermophilic Species from Hot Springs. *International Journal of Systematic and Evolutionary Microbiology* **1997**, *47* (4), 939–947. https://doi.org/10.1099/00207713-47-4-939.
(32) Uddin, K. M.; Almatarneh, M. H.; Shaw, D. M.; Poirier, R. A. Mechanistic Study of the Deamination Reaction of Guanine: A Computational Study. *J. Phys. Chem. A* **2011**, *115* (10), 2065–2076. https://doi.org/10.1021/jp1120806.
(33) Fateev, I. V.; Kharitonova, M. I.; Antonov, K. V.; Konstantinova, I. D.; Stepanenko, V. N.; Esipov, R. S.; Seela, F.; Temburnikar, K. W.; Seley-Radtke, K. L.; Stepchenko, V. A.; Sokolov, Y. A.; Miroshnikov, A. I.; Mikhailopulo, I. A. Recognition of Artificial Nucleobases by E. Coli Purine Nucleoside Phosphorylase versus Its Ser90Ala Mutant in the Synthesis of Base-Modified Nucleosides. *Chemistry – A European Journal* **2015**, *21* (38), 13401–13419. https://doi.org/10.1002/chem.201501334.
(34) Kulikova, I. V.; Drenichev, M. S.; Solyev, P. N.; Alexeev, C. S.; Mikhailov, S. N. Enzymatic Synthesis of 2-Deoxyribose 1-Phosphate and Ribose 1 Phosphate and Subsequent Preparation of Nucleosides. *European Journal of Organic Chemistry* **2019**, *2019* (41), 6999–7004. https://doi.org/10.1002/ejoc.201901454.
(35) Varizhuk, I. V.; Oslovsky, V. E.; Solyev, P. N.; Drenichev, M. S.; Mikhailov, S. N. Synthesis of α-D-Ribose 1-Phosphate and 2-Deoxy-α-D-Ribose 1-Phosphate Via Enzymatic Phosphorolysis of 7-Methylguanosine and 7-Methyldeoxyguanosine. *Current Protocols* **2022**, *2* (1), e347. https://doi.org/10.1002/cpz1.347.